Journal of Economic Entomology, 114(5), 2021, 1975–1982
https://doi.org/10.1093/jee/toab155
Advance Access Publication Date: 12 August 2021
Research

ENTOMOLOGICAL SOCIETY OF AMERICA
SHARING INSECT SCIENCE GLOBALLY

OXFORD

Beneficial Uses of Insects

A Gut-Specific *LITAF*-Like Gene in *Antheraea pernyi* (Lepidoptera: Saturniidae) Involved in the Immune Response to Three Pathogens

Yuyu Lei,[1,*] Ying Li,[1,*] Xinfeng Yang,[2,*] Xuwei Zhu,[2] Xian Zhang,[1] Jie Du,[1] Shimei Liang,[1] Shanshan Li,[1] and Jianping Duan[1,3,]

[1]Henan Key Lab of Funiu Mountain Insect Biology, College of Life Science and Agricultural Engineering, Nanyang Normal University, Nanyang 473061, PR China, [2]Lab of Tussah Genetics and Breeding, Henan Institute of Sericulture Science, Zhengzhou 450008, PR China, and [3]Corresponding author, e-mail: djping8199@nynu.edu.cn

*These authors have contributed equally to this work.

Subject Editor: Yan-Qun Liu

Received 21 April 2021; Editorial decision 27 June 2021

Abstract

Antheraea pernyi (Guérin-Méneville 1855) is an important resource for silk, food, and biohealth products; however, exogenous pathogens largely affect the commercial application potential of this species. Since the gut is a key organ for the digestion and absorption of nutrients as well as for immune defense, we used comparative transcriptome analysis to screen for a gut-specific molecular tool for further functional research in *A. pernyi*. In total, 3,331 differentially expressed genes (DEGs) were identified in the gut compared with all other pooled tissues of *A. pernyi*, including 1,463 upregulated genes in the gut. Among these, we further focused on a lipopolysaccharide-induced tumor necrosis factor-α factor (*LITAF*) gene because of its high gut-specific expression and the presence of a highly conserved SIMPLE-like domain, which is related to the immune response to pathogenic infections in many species. The cDNA sequence of *ApLITAF* was 447-bp long and contained a 243-bp open reading frame encoding an 80-amino acid protein. Immune challenge assays indicated that *ApLITAF* expression was significantly upregulated in the gut of *A. pernyi* naturally infected with nucleopolyhedrovirus (NPV) or fed leaves infected with the gram-negative bacterium *Escherichia coli* (Migula 1895) and the gram-positive bacterium *Bacillus subtilis* (Ehrenberg 1835). Cell transfection showed that ApLITAF localized to the lysosome. Collectively, these results suggested that *ApLITAF* played a role in the immune response of *A. pernyi* and could facilitate the future research and breeding application in this species.

Key words: *Antheraea pernyi*, lipopolysaccharide-induced tumor necrosis factor-α factor-like gene, immune response, differentially expressed gene, gut-specific gene

Antheraea pernyi (Guérin-Méneville 1855) is an economically important lepidopteran insect that is valuable for silk production, food consumption, and biomedical applications (Li et al. 2017, Silva et al. 2019). The larvae of *A. pernyi* are commercially cultivated on *Quercus* leaves outdoors, where they inevitably are exposed to a wide array of pathogens, including bacteria, viruses, fungi, and microsporidia (Hillyer 2016, Sun et al. 2017). Many of these pathogens infect *A. pernyi* through an oral transmission route during the ingestion of leaves. Once these pathogens successfully colonize the gut of *A. pernyi*, resulting in detrimental effects, infections are rapidly transmitted, leading to outbreaks of silkworm disease and ultimately causing serious economic losses. Because the gut of *A. pernyi* is regarded as the first line of defense against various orally transmitted pathogens (Liu et al. 2020b), inhibition of the invasion, replication, and transmission of pathogens in the gut would be an appropriate strategy for enhancing the disease resistance capacity of *A. pernyi*.

Many tissue-specific proteins, including lipase-1 (Ponnuvel et al. 2003), serine protease-2 (Nakazawa et al. 2004), NADPH oxidoreductase (Selot et al. 2007), and serine protease-36 (Liu et al. 2017), have been shown to have strong digestive or immune activity

in the gut of *Bombyx mori* (Linnaeus 1758). Transgenic expression of lipase and peptidoglycan recognition protein genes in the gut of *B. mori* is an effective disease-resistance strategy against exogenous pathogens (Jiang et al. 2013, Zhao et al. 2018). Although the innate immune mechanisms of these two silkworms are highly similar (Sun et al. 2016, Wang et al. 2018, Jiang 2021), and some immune-related genes have already been identified in *A. pernyi* (Kausar et al. 2018, Liu et al. 2018, Zhang et al. 2019), it is difficult to achieve disease-resistance breeding in *A. pernyi* because of a lack of gut-specific molecular tools.

Microarray-based gene expression data have been used to identify tissue-specific genes in *B. mori* (Xia et al. 2007, Park et al. 2010). Despite the lack of genome-wide microassays specific to *A. pernyi*, the recent chromosome-scale genome assembly of *A. pernyi* (Duan et al. 2020) may facilitate the development of useful molecular tools based on the genome-wide screening of tissue-specific gene expression using low-cost, advanced comparative transcriptome sequencing techniques.

Lipopolysaccharide-induced tumor necrosis factor-α factor (*LITAF*) was first identified in human cell lines (Myokai et al. 1999) and was subsequently shown to be involved in innate immune response in many species (Moriwaki et al. 2001, Smith et al. 2012, Wang et al. 2012, Jeong et al. 2015, Liu et al. 2020a). Members of the LITAF family typically contain the PPXY motif in the N-terminus and SIMPLE-like domain (SLD) in the C-terminus. Some LITAF family members, which lack the PPXY motif, can interact with PPXY-containing LITAFs to colocalize at late endosomes/lysosomes (Eaton et al. 2013). Therefore, in this study, we screened for a gut-specific *LITAF* gene in *A. pernyi* by identifying differentially expressed genes (DEGs) in the gut and other tissues. We functionally analyzed the *LITAF* gene in *A. pernyi* with an immune challenge experiment using three types of pathogens: nucleopolyhedrovirus (NPV), the gram-negative bacterium *Escherichia coli*, and the gram-positive bacterium *Bacillus subtilis*. Our findings provided a new tool for future research to better understand the interactions between *A. pernyi* and exogenous pathogens, identify resistance mechanisms, and ultimately expand the commercial application of this economically valuable species.

Materials and Methods

Insects and Tissue Samples

The larvae of the Yuda strain were fed on fresh *Quercus* leaves outdoors in the oak silkworm base of Henan Institute of Sericulture Science, Zhengzhou, China. The gut and other pooled tissues from three fifth-instar larvae were prepared for comparative transcriptome sequencing. Each sample was evaluated using three biological replicates. Tissues of the two sexes were also dissected separately from five individuals for the analysis of gene expression.

Comparative Transcriptome

Total RNA was extracted from the gut and the remaining pooled tissues (rest-PT) using TRIzol Reagent (Invitrogen, USA) and further purified using RNeasy mini kits (Qiagen, Australia). RNA concentration was measured using a Qubit 2.0 Flurometer (Invirogen). Two micrograms of RNA per sample was applied for sequencing library preparation using a VAHTS mRNA-seq V2 Library Prep Kit (Vazyme, China). Briefly, RNA samples were purified using mRNA Capture Beads to remove ribosomal RNA. The purified RNA was fragmented using Frag/Prime Buffer at 94℃ for 8 min, followed by a hold at 4℃. The fragmented mRNA was immediately reverse-transcribed with random primers, followed by second-strand synthesis to produce cDNA fragments. Subsequently, the ends of double-stranded cDNA were repaired and cleaned using End Prep Mix and DNA Clean Beads, respectively. The resulting double-stranded cDNA was ligated with adaptors and cleaned again. The cleaned double-stranded cDNA was amplified and purified to yield the final sequencing library. After the assessment of library quality using a Bioanalyzer 2100 system (Agilent), the library was sequenced on the Illumina HiSeq 2500 platform (Illumina), generating 150 bp paired-end reads.

Read quality was controlled using the Trimmomatic v0.36 program, with default settings (Bolger et al. 2014). Qualified reads were used for a comprehensive assembly using Trinity v2.4.0 with default parameters (Haas et al. 2013), followed by transcript alignment and quantification with Bowtie2 v2.3.2 (Langmead and Salzberg 2012) and Salmon v0.8.2 (Patro et al. 2017) software, respectively. The DEGSeq R package (release 1.30.1) was used to identify significant DEGs between the gut and rest-PT according to a corrected *P*-value of 0.05 and $\log_2$ fold-change of ±1 (Love et al. 2014).

The DEGs identified in the gut of *A. pernyi* were annotated using the NCBI BLAST+ v2.60 tool (Altschul et al. 1997) with an e-value threshold of 1e-5 against the CDD (Marchler-Bauer et al. 2013), KOG (Tatusov et al. 2000), PFAM (Finn et al. 2016), UniProt (UniProt-Consortium 2019), NR, and NT (http://ncbi.nlm.nih.gov/) databases (Supp Table S1 [online only]). The resulting UniProt annotations were converted into Gene Ontology annotations. The automatic Kyoto Encyclopedia of Genes and Genomes (KEGG) annotation server KASS (Moriya et al. 2007) was used to infer significantly enriched KEGG pathways with default parameters.

Reverse Transcription Polymerase Chain Reaction (RT–PCR) Expression Analysis

Total RNA was extracted from the head, integument, gut, silk glands, Malpighian tubules, hemocytes, and remaining mixed tissues from the two sexes using TRIzol reagent (Invitrogen). The cDNA templates were synthesized using a BeyoRT II cDNA Synthesis Kit with gDNA Eraser (Beyotime, China). RT–PCR was performed using 2× EasyTaq PCR SuperMix (+dye) (TransGen, China) to detect the expression levels of selected genes with high and exclusive expression in the gut using the primer sets and annealing temperatures shown in Supp Table S2 (online only). The housekeeping ribosomal protein gene of *A. pernyi* (*ApL32*) was used as a reference gene to standardize the variance among samples. The PCR conditions were as follows: 95°C for 3 min; 30 cycles of 95°C for 15 s, annealing temperature for 20 s, and 72°C for 1 min; final extension for 5 min at 72°C.

Rapid Amplification of cDNA Ends Cloning and Sequence Analysis

Random amplification of cDNA ends was carried out as described previously (Duan et al. 2013b) for the two terminal regions of the *Apm8* gene, which showed gut-specific expression in *A. pernyi* and was annotated to have potential immune function. All fragments were sequenced and assembled for the full-length mRNA of *Apm8*.

The open reading frame (ORF) of full-length mRNA was analyzed using ORF Finder (https://www.ncbi.nlm.nih.gov/orffinder/). The amino acid sequence was derived and predicted for a consensus domain using SMART (http://smart.embl-heidelberg.de/). The deduced amino acid sequence was searched against the NR database for related homologs using the Blastp algorithm. Multiple sequence alignment of the deduced protein with related homologs was performed using ClustalW (Thompson et al. 2002). The phylogenetic relationships were determined using the neighbor-joining method

in the MEGA program (Kumar et al. 2018) with 1,000 bootstrap replications. Based on these results, *Apm8* showed high homology to *LITAF*, and was therefore designated *ApLITAF* and subjected to further molecular and functional characterization.

Immune Challenge

Fifth-instar newly molted larvae of *A. pernyi* were starved for 1 d and then used for the immune challenge experiment. To simulate natural infection, fresh *Quercus* leaves were briefly submerged in solutions of *E. coli* and *B. subtilis* (1×10^9 cells/mL) and then used to feed the hungry larvae, respectively. Larvae were maintained separately in individual partitions, and each larva was fed the same amount of leaves. After all of the leaves had been eaten, the larvae were transferred to healthy leaves, and the time was started. The guts were dissected at 8 and 14 h postinfection (hpi) and frozen in liquid nitrogen for RNA extraction. The guts of fifth-instar larvae naturally infected with NPV based on physical symptoms were also dissected for RNA extraction. The cDNA templates were prepared as described above for quantitative PCR. Each assay was carried out in triplicate. Student's *t*-test was invoked to assess the significant difference. The primer sets for the *A. pernyi actin* and glyceraldehyde 3-phosphate dehydrogenase (*GAPDH*) genes were used as the references for relative quantification.

Lyso-Tracker Red and 4′,6-diamidino-2-phenylindole (DAPI) Staining in Cells Expressing *ApLITAF*

The ORFs of the *ApLITAF* and enhanced green fluorescent protein (*EGFP*) genes were amplified from the *A. pernyi* gut cDNA and the pBac[3×p3 EGFP afm] construct (Duan et al. 2013a), respectively. The two fragments were assembled together into the vector 1180A3-ser1pA by homologous recombination using NEBuilder HiFi DNA Assembly Master Mix (NEB, USA), producing 1180A3ApLITAFEGFPser1pA (named 1LITAF-G), a fused expression vector of *ApLITAF* with *EGFP*.

1LITAF-G was transfected into BmN cells, a *B. mori* ovary cell line (Pan et al. 2010). The cells were then stained with Lyso-Tracker Red (Beyotime, China) for 1 h at 72 h posttransfection. Cells were washed three times in phosphate-buffered saline and then incubated with 30% DAPI (Beyotime, China) for 15 min at 28°C. Following three washes in phosphate-buffered saline, the cells were fixed for 20 min in 4% paraformaldehyde (Solarbio, China). The cells were mounted with an antifade mounting medium (Solarbio, China) and directly observed under a TE2000-E laser confocal microscope (Nikon, Japan).

Results

Screening for Gut-specific Candidate Genes

RNA sequencing and data processing identified 3,331 DEGs between the *A. pernyi* gut and other pooled tissues (rest-PT; Supp Table S1 [online only]), including 1,468 upregulated and 1,868 downregulated genes in the gut (Fig. 1A and Supp Fig. S1 [online only]).

Considering the possible difference between the results of transcriptomic analysis and the actual expression characteristics of some genes, three criteria were applied to further screen candidate

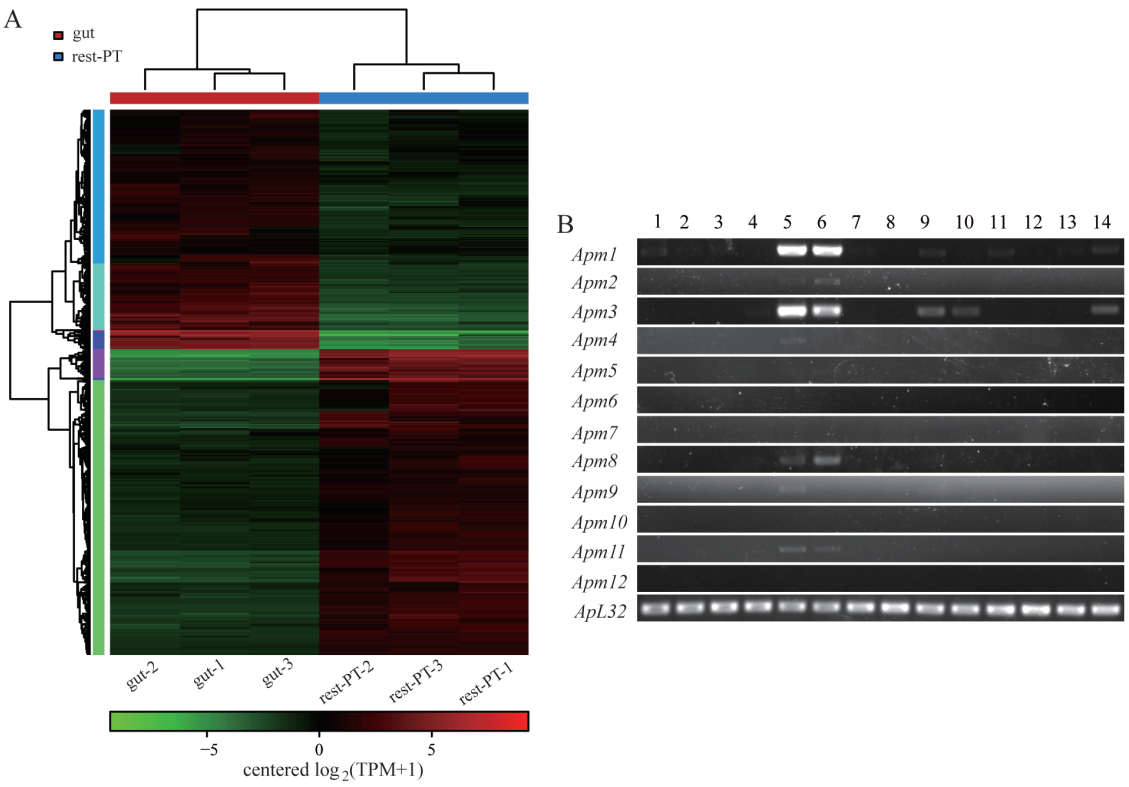

Fig. 1. Large-scale transcriptome screening of gut-specific candidate genes in *A. pernyi*. (A) Hierarchical clustering of the differentially expressed genes (DEGs) between the gut and remaining pooled tissues (rest-PT). (B) RT–PCR analysis of the expression of 12 potentially gut-specific DEGs. *ApL32* was used as an internal control. Primer sets are shown in Supp Table S2 (online only), and the details of gene numbers are given in Supp Table S3 (online only). Lanes: 1 and 2, head; 3 and 4, integument; 5 and 6, gut; 7 and 8, silk glands; 9 and 10, Malpighian tubules; 11 and 12, hemocytes; 13 and 14, remaining mixed tissues. Odd and even numbers indicate female and male tissues, respectively.

genes: (1) they were included in the 1,468 upregulated gene set, (2) they had higher read counts in the gut, and (3) they had not been sequenced and had zero read counts in the rest-PT. After filtering, the remaining genes were sorted by their read counts, and the top 12 genes (Supp Table S3 [online only]) were selected to further detect their expression in different tissues of female and male *A. pernyi*. RT–PCR showed that five genes (*Apm5*, *Apm6*, *Apm7*, *Apm10*, and *Apm12*) were not expressed in any tissue, and two genes (*Apm1* and *Apm3*) had relatively high expression levels in the gut compared with those in the other tissues (Fig. 1B). Three of these genes (*Apm4*, *Apm8*, and *Apm11*) were exclusively expressed in the gut.

Functional annotation suggested that *Apm4*, *Apm8*, and *Apm11* were members of the oxidoreductase, LITAF, and carboxylic esterase families, respectively (Supp Table S2 [online only]). Because members of the LITAF family have been reported to participate in the innate immune response against exogenous pathogens in many species (Moriwaki et al. 2001, Smith et al. 2012, Wang et al. 2012, Jeong et al. 2015, Liu et al. 2020a), we designated *Apm8* as *ApLITAF* and focused on this gene for subsequent experiments.

Sequence Analysis of *ApLITAF*

To determine the characteristics of the *ApLITAF* sequence, its full-length mRNA was first cloned using RT–PCR and then 5′- and 3′-RACE (Fig. 2). The assembled mRNA sequence of *ApLITAF* contained 447 nucleotides, with a 72-bp 5′-untranslated region, a 132-bp 3′-untranslated region, and a 243-bp ORF encoding 80 amino acid residues. A BLAST search of the *ApLITAF* mRNA sequence against the complete *A. pernyi* genome showed that *ApLITAF* was

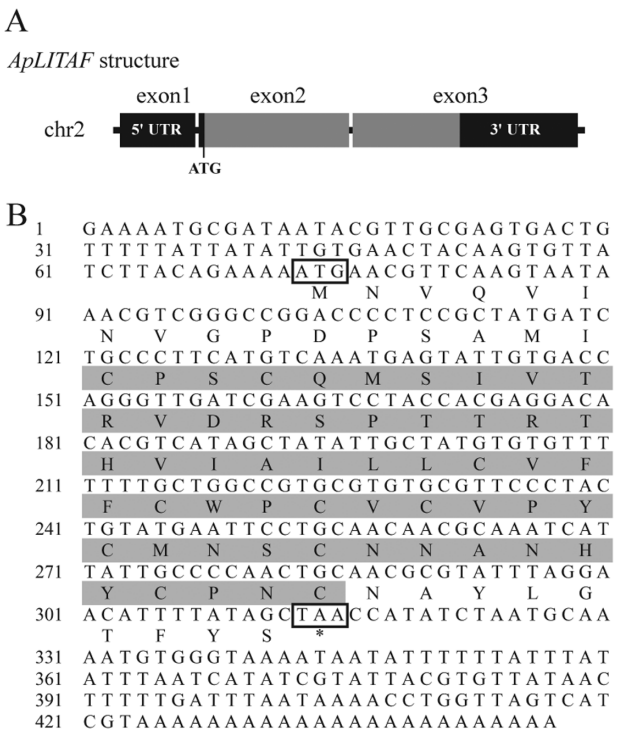

Fig. 2. Detailed information of the gut-specific *ApLITAF* gene. (A) The gene model of *ApLITAF*, corresponding to *Apm8* in Fig. 1B. The black boxes show the 5′- and 3′-untranslated regions. The gray box is the open reading frame. (B) Nucleotide and deduced amino acid sequences of *ApLITAF*. The start codon ATG and termination codon TAA are boxed. The numbers of nucleotides are shown to the left of the sequence. The shaded amino acids represent a modified RING-finger domain, which is interrupted by a hydrophobic stretch and designated as the SLD domain in Fig. 3.

located on chromosome 2 (chr2) and contained three exons (Fig. 2A). The calculated molecular mass of 8,901 Da indicated that *ApLITAF* encoded a small-molecule protein.

Alignment of the ApLITAF amino acid sequence with its homologs showed striking sequence identity with the C-terminus of LITAFs from insects, *Mollusca*, and vertebrates (Fig. 3). The C-terminus of ApLITAF also contained an SLD domain, including all three representative motifs (a CXXC motif, hydrophobic stretch, and HXCXXC motif), whereas the N-terminus of LITAF was missing in ApLITAF, including the typical PPXY motif.

To assess the evolutionary relationship between ApLITAF and LITAFs in *Mollusca*, vertebrates, and other insects, a phylogenetic tree was constructed (Fig. 4). The results revealed that LITAF members could be classified into three clearly separated clades. The first clade was formed by dipteran and lepidopteran LITAFs, which were also clearly divided. ApLITAF clustered in the Lepidoptera group, indicating its closer evolutionary origin with other lepidopteran LITAFs.

Expression of *ApLITAF* in the Gut of *A. pernyi* After Immune Challenge

To determine whether the ApLITAF protein was involved in biotic stress, the expression of *ApLITAF* in the gut of *A. pernyi* was examined using quantitative PCR. Challenge of fifth-instar larvae with *E. coli* and *B. subtilis* by oral infection led to considerably upregulated expression of *ApLITAF* (Fig. 5A), although the induction strength varied according to the pathogen type. At 8 hpi, *ApLITAF* expression was not induced by *E. coli*, but was significantly triggered by *B. subtilis*. At 14 hpi, both *E. coli* and *B. subtilis* significantly induced *ApLITAF* upregulation, although the extent of change was greater with *B. subtilis*.

NPV is the most dangerous pathogen for *A. pernyi* sericulture. NPV-infected *A. pernyi* showed circular pus blotches of various sizes on the integument (Fig. 5B), ultimately leading to death. In NPV-infected *B. mori*, the gene expression of actin was affected, whereas that of *GAPDH* was relatively steady (Guo et al. 2016). Accordingly, we used both these reference genes to assess the expression levels of *ApLITAF* in larvae naturally infected with NPV. The results showed that the expression of *ApLITAF* was significantly increased under the two reference conditions (Fig. 5C and 5D).

ApLITAF Localizes in Lysosome

The cellular localization of some proteins can often reveal their potential biological functions. Therefore, to determine the subcellular localization of ApLITAF, we transiently transfected 1LITAF-G into BmN cells; green fluorescence indicated the cellular localization. ApLITAF exhibited a punctate staining pattern, which overlapped with the pattern of the lysosome marker Lyso-Tracker Red (Fig. 6). Therefore, we concluded that ApLITAF localized to the lysosome in BmN cells.

Discussion

A. pernyi plays an important role in the development of sericulture. However, every year, silkworm diseases cause serious economic losses. Oral infection is the main mechanism through which exogenous pathogens colonize *A. pernyi*. Therefore, the gut is the most important organ to target for preventing the invasion, replication, and transfer of pathogens. Although the complete *A. pernyi* genome has been published (Duan et al. 2020), additional disease-resistance research on this economically important insect has been limited by a lack of useful molecular tools.

Fig. 3. Multiple sequence alignment of ApLITAF with its homologs from insects, *Mollusca,* and vertebrates. The black line indicates the conserved SLD domain. The red line shows the hydrophobic stretch. The two motifs (CXXC and HXCXXC) are marked using red capitals. The PPXY motifs in the N-terminus are shown in green boxes. ApLITAF, *Antheraea pernyi* LITAF; BmLITAF, *Bombyx mori* XP_021204897.1; BmLITAF-X1, *Bombyx mori* XP_021204685.1; BmLITAF-X2, *Bombyx mori* XP_004927943.1; BmaLITAF, *Bombyx mandarina* XP_028028595.1; SlLITAF, *Spodoptera litura* XP_022829186.1; PmLITAF, *Papilio machaon* KPJ20400.1; TnLITAF-X1, *Trichoplusia ni* XP_026746530.1; TnLITAF-X2, *Trichoplusia ni* XP_026746536.1; HaLITAF-s, *Helicoverpa armigera* XP_021193243.1; HaLITAF-l, *Helicoverpa armigera* XP_021195218.1; PxLITAF, *Papilio xuthus* KPI91185.1; GmLITAF, *Galleria mellonella* XP_031763557.1; AhLITAF, *Aphantopus hyperantus* XP_034825472.1; OfLITAF-s, *Ostrinia furnacalis* XP_028171762.1; OfLITAF-l, *Ostrinia furnacalis* XP_028171761.1; VtLITAF, *Vanessa tameamea* XP_026491413.1; AalboLITAF, *Aedes albopictus* XP_029721827.1; AaeLITAF-s, *Aedes aegypti* XP_001652694.2; AaeLITAF-l, *Aedes aegypti* XP_001652693.2; AalbiLITAF, *Anopheles albimanus* XP_035774144.1; CcLITAF, *Cipangopaludina chinensis* AEX08893.1; CgLITAF, *Crassostrea gigas* ABO70331.1; TgLITAF, *Tegillarca granosa* QFP12293.1; SgLITAF, *Solen grandis* AEW43450.1; AfLITAF, *Azumapecten farreri* ABI79459.1; HsLITAF, *Homo sapiens* AAH00053.1; MmLITAF, *Mus musculus* NP_064364.1; RnLITAF, *Rattus norvegicus* NP_001099205.1; XlLITAF, *Xenopus laevis* NP_001089805.1; GgLITAF, *Gallus gallus* NP989598.1; DrLITAF, *Danio rerio* NP_001002184.1.

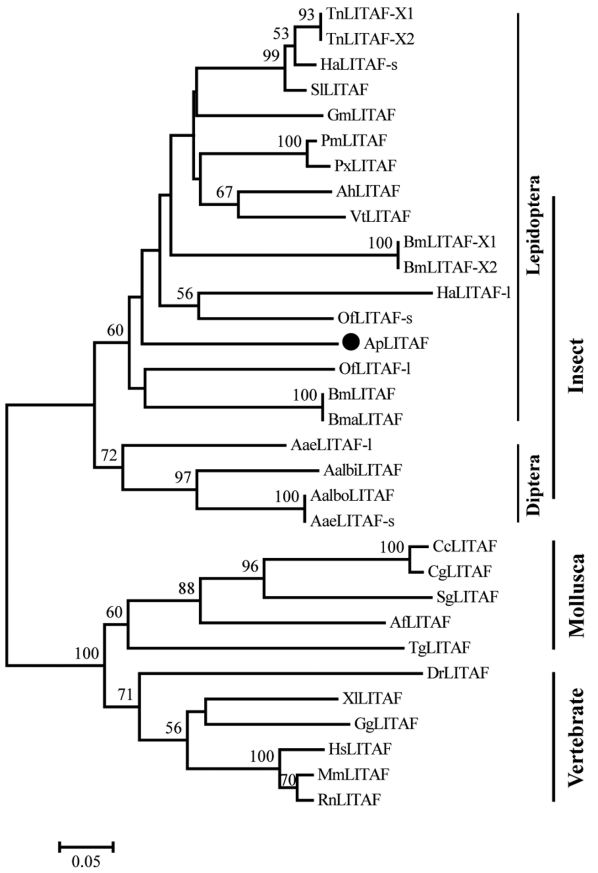

Fig. 4. Neighbor-joining phylogenetic tree of ApLITAF with its homologs from insects, *Mollusca,* and vertebrates. Numbers represent the bootstrap values (percentages) from 1,000 replicates. The LITAF from *A. pernyi* is marked with a solid circle.

In this study, we screened out a *LITAF*-like gene with gut-specific expression in *A. pernyi* through large-scale, low-cost transcriptome analysis and demonstrated its significant response patterns to the gram-negative bacterium *E. coli*, gram-positive bacterium *B. subtilis*, and NPV. Gut-specific genes have been identified and used for disease resistance research in domesticated silkworms (Jiang et al. 2013, Zhao et al. 2018). To date, no gut-specific genes in *A. pernyi* have been identified and exploited. Here, we found that *ApLITAF* may have applications in the development of a useful molecular tool in the breeding of novel strains with large-scale disease-resistance capacity.

The characteristics and immune function of LITAFs have been extensively demonstrated in many other species (Supp Fig. S2 [online only]), including humans (Moriwaki et al. 2001), mice (Han et al. 2007), *Crassostrea gigas* (Park et al. 2008), *Litopenaeus vannamei* (Wang et al. 2012), *Anopheles gambiae* (Smith et al. 2012), *Brachionus koreanus* (Jeong et al. 2015), and *Tegillarca granosa* (Liu et al. 2020a); however, to the best of our knowledge, the characteristics and immune functions of LITAFs in silkworms have not been reported previously. Here, the full-length mRNA of the *LITAF* gene was first cloned in *A. pernyi* using sequence analysis. Multiple sequence alignment revealed that the C-terminus of LITAFs was variable, but showed some common features among species, including the CXXC and HXCXXC motifs and the hydrophobic stretch in the SLD domain. The phylogenetic tree further provided evidence that the encoded protein clustered into the Lepidoptera group of the LITAF family. These observations prompted us to conclude that this mRNA was transcribed from a *LITAF* gene.

The specific expression of *ApLITAF* in the digestive and immune-related organ (i.e., the gut), as the key route for the pathogen to invasion, indicates its potential role in biotic stress in *A. pernyi*. The significant upregulation of *ApLITAF* upon immune challenge by different pathogens suggested that the functions of the LITAF family were highly conserved and that ApLITAF may play important roles in *A. pernyi* immunity. However, the

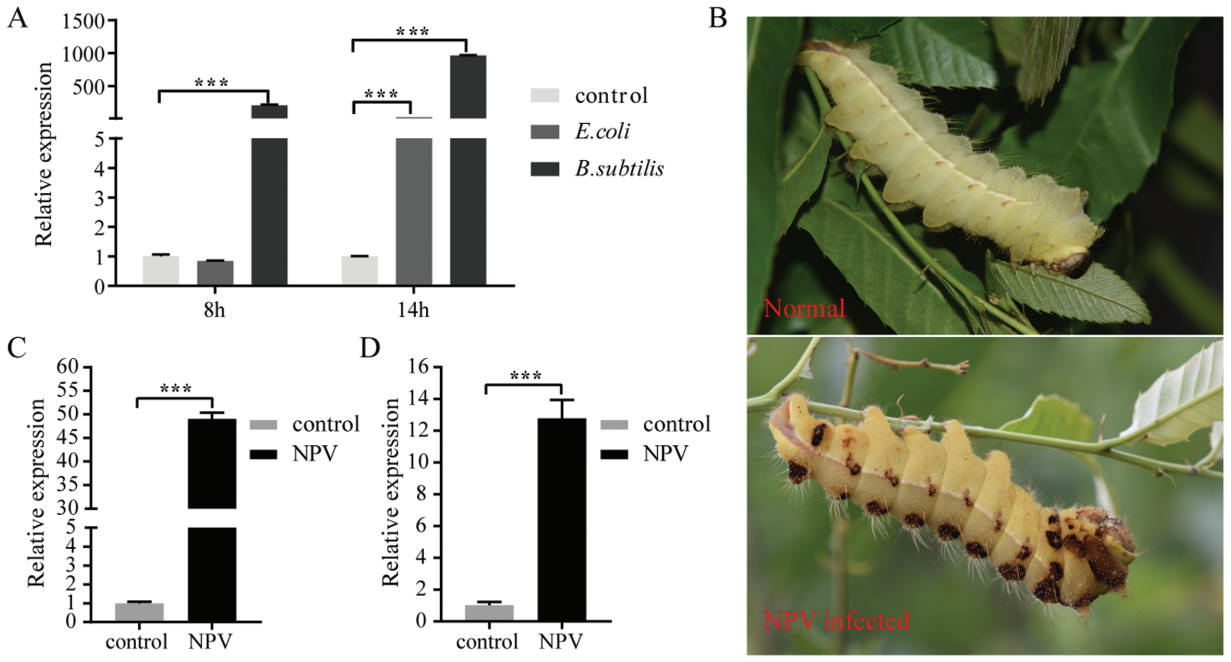

Fig. 5. Expression pattern of *ApLITAF* in the gut of *A. pernyi* orally infected with three types of pathogens. (A) Changes in the expression of *ApLITAF* induced by the gram-negative bacterium *E. coli* and the gram-positive bacterium *B. subtilis.* (B) Phenotypic changes occurring at the later stage of natural infection with NPV. (C) *ApLITAF* upregulation induced by NPV using *ApActin* as the control. (D) *ApLITAF* upregulation triggered by NPV; *ApGAPDH* served as the control. ***$P < 0.001$, Student's *t*-test.

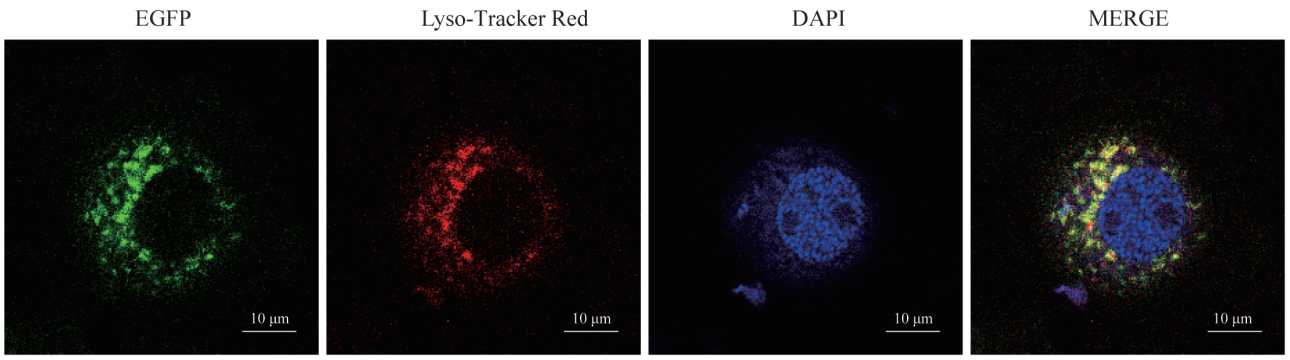

Fig. 6. Cellular localization of ApLITAF. The fused protein of LITAF and EGFP is shown in green. A lysosome marker (Lyso-Tracker Red) was applied to live cells at 72 h post-transfection (hpt) to visualize the lysosome (red). The nucleus was visualized using DAPI staining (blue).

underlying mechanisms mediating the expression of this protein in response to different pathogen types remain unclear. Infection by gram-negative bacteria usually activates the Imd pathway, whereas the Toll-like receptor (TLR) pathway typically responds to gram-positive bacteria (Jiang 2021). The lipopolysaccharide-induced TLR pathway (LPS/TLR2,4/MyD88) can promote LITAF phosphorylation and nuclear translocation in mouse macrophages (Tang et al. 2006), indicating that ApLITAF may be a member of the TLR pathway in *A. pernyi*. However, *MyD88* was not expressed in the gut of *A. pernyi* (Sun et al. 2016); accordingly, further studies are needed to identify the pathway through which ApLITAF participates.

LITAFs generally localize along secretory and lysosomal degradation pathways, which are mediated by the PPXY motif in the N-terminus of the protein (Eaton et al. 2011). However, the N-terminus of ApLITAF is very short and has no PPXY motif. Similar LITAFs were also identified in *Anopheles gambiae* (AgLL3; Supp Fig. S2 [online only]) and frog virus 3 (FV3_75L; Supp Fig. S3 [online only]). AgLL3 plays an important role in limiting *Plasmodium* infection (Smith et al. 2012), whereas FV3 is a virus that infects *Xenopus laevis*. The interaction between FV3_75L and *X. laevis* LITAF, mediated through their SLD domains, can alter the subcellular localization of FV3_75L from the early to late endosomes (Eaton et al. 2013). Although ApLITAF has also been shown to localize to the lysosomes in BmN cells, further studies are required to elucidate its function in the lysosomal pathway. Because a LITAF with the PPXY motif was identified in *A. pernyi* (Supp Fig. S4 [online only]), evaluation of the putative interaction between this member and ApLITAF may provide insights into its functions. Further evidence is needed to clarify this hypothesis. Although the specific role is currently unclear, our results suggest that the molecular functions of ApLITAF may be related to the lysosomal pathway.

In conclusion, we provided evidence for a novel component associated with the response of *A. pernyi* to pathogens, offering an important starting point for additional investigations of the mechanisms underlying the roles of ApLITAF. Further elucidation of these roles and the characterization of other gut-specific genes may establish effective strategies for improving the evaluation and application of *A. pernyi* genes.

Supplementary Data

Supplementary data are available at *Journal of Economic Entomology* online.

Acknowledgments

We are thankful to the annonymous reviewers and editors for their insightful comments and suggestions. This work was supported by National Natural Science Foundation of China, Scientific and Technological Project of Henan Province (No. 202102110200 and No. 182102310077) and Science Foundation of Nanyang Normal University (No. 2018ZX011).

Data Accessibility

The raw data have been deposited in the Genome Sequence Archive (GSA) (http://gsa.big.ac.cn/) in China National Center for Bioinformation, National Genomics Data Center (CNCB-NGDC), Beijing Institue of Genomics, Chinese Academic of Sciences, under accession number CRA004300.

References Cited

Altschul, S. F., T. L. Madden, A. A. Schäffer, J. Zhang, Z. Zhang, W. Miller, and D. J. Lipman. 1997. Gapped BLAST and PSI-BLAST: a new generation of protein database search programs. Nucleic Acids Res. 25: 3389–3402.

Bolger, A. M., M. Lohse, and B. Usadel. 2014. Trimmomatic: a flexible trimmer for Illumina sequence data. Bioinformatics. 30: 2114–2120.

Duan, J., H. Xu, S. Ma, H. Guo, F. Wang, P. Zhao, and Q. Xia. 2013a. Cre-mediated targeted gene activation in the middle silk glands of transgenic silkworms (*Bombyx mori*). Transgenic Res. 22: 607–619.

Duan, J., H. Xu, F. Wang, S. Ma, X. Zha, H. Guo, P. Zhao, and Q. Xia. 2013b. Novel female-specific trans-spliced and alternative splice forms of dsx in the silkworm *Bombyx mori*. Biochem. Biophys. Res. Commun. 431: 630–635.

Duan, J., Y. Li, J. Du, E. Duan, Y. Lei, S. Liang, X. Zhang, X. Zhao, Y. Kan, L. Yao, *et al.* 2020. A chromosome-scale genome assembly of *Antheraea pernyi* (Saturniidae, Lepidoptera). Mol. Ecol. Resour. 20: 1372–1383.

Eaton, H. E., G. Desrochers, S. B. Drory, J. Metcalf, A. Angers, and C. R. Brunetti. 2011. SIMPLE/LITAF expression induces the translocation of the ubiquitin ligase itch towards the lysosomal compartments. Plos One. 6: e16873.

Eaton, H. E., A. Ferreira Lacerda, G. Desrochers, J. Metcalf, A. Angers, and C. R. Brunetti. 2013. Cellular LITAF interacts with frog virus 3 75L protein and alters its subcellular localization. J. Virol. 87: 716–723.

Finn, R. D., P. Coggill, R. Y. Eberhardt, S. R. Eddy, J. Mistry, A. L. Mitchell, S. C. Potter, M. Punta, M. Qureshi, A. Sangrador-Vegas, *et al.* 2016. The Pfam protein families database: towards a more sustainable future. Nucleic Acids Res. 44: D279–D285.

Guo, H., L. Jiang, and Q. Xia. 2016. Selection of reference genes for analysis of stress-responsive genes after challenge with viruses and temperature changes in the silkworm *Bombyx mori*. Mol. Genet. Genomics. 291: 999–1004.

Haas, B. J., A. Papanicolaou, M. Yassour, M. Grabherr, P. D. Blood, J. Bowden, M. B. Couger, D. Eccles, B. Li, M. Lieber, *et al.* 2013. De novo transcript

sequence reconstruction from RNA-seq using the Trinity platform for reference generation and analysis. Nat. Protoc. 8: 1494–1512.

Han, S., K. Lee, J. Yeo, H. Kweon, S. Woo, M. Lee, H. Baek, S. Kim, and K. Park. 2007. Effect of honey bee venom on microglial cells nitric oxide and tumor necrosis factor-alpha production stimulated by LPS. J. Ethnopharmacol. 111: 176–181.

Hillyer, J. F. 2016. Insect immunology and hematopoiesis. Dev. Comp. Immunol. 58: 102–118.

Jeong, C. B., J. H. Lee, J. S. Lee, and J. S. Rhee. 2015. Early expansion and expression of the lipopolysaccharide (LPS)-induced TNF-α factor (LITAF) gene family in the LPS-exposed monogonont rotifer *Brachionus koreanus*. Comp. Biochem. Physiol. B. Biochem. Mol. Biol. 188: 15–23.

Jiang, L. 2021. Insights into the antiviral pathways of the silkworm *Bombyx mori*. Front. Immunol. 12: 639092.

Jiang, L., P. Zhao, T. Cheng, Q. Sun, Z. Peng, Y. Dang, X. Wu, G. Wang, S. Jin, P. Lin, *et al*. 2013. A transgenic animal with antiviral properties that might inhibit multiple stages of infection. Antiviral Res. 98: 171–173.

Kausar, S., M. N. Abbas, C. Qian, B. Zhu, J. Gao, Y. Sun, L. Wang, G. Wei, and C. Liu. 2018. Role of *Antheraea pernyi* serpin 12 in prophenoloxidase activation and immune responses. Arch Insect Biochem Physiol 97:e21435.

Kumar, S., G. Stecher, M. Li, C. Knyaz, and K. Tamura. 2018. MEGA X: molecular evolutionary genetics analysis across computing platforms. Mol. Biol. Evol. 35: 1547–1549.

Langmead, B., and S. L. Salzberg. 2012. Fast gapped-read alignment with Bowtie 2. Nat. Methods. 9: 357–359.

Li, W., Z. Zhang, L. Lin, and O. Terenius. 2017. *Antheraea pernyi* (Lepidoptera: Saturniidae) and its importance in sericulture, food consumption, and traditional Chinese medicine. J. Econ. Entomol. 110: 1404–1411.

Liu, H. W., Y. S. Li, X. Tang, P. C. Guo, D. D. Wang, C. Y. Zhou, Q. Y. Xia, and P. Zhao. 2017. A midgut-specific serine protease, BmSP36, is involved in dietary protein digestion in the silkworm, *Bombyx mori*. Insect Sci. 24: 753–767.

Liu, Q. N., Y. Liu, Z. Z. Xin, X. Y. Zhu, B. M. Ge, C. F. Li, D. Wang, X. G. Bian, L. Yang, L. Chen, *et al*. 2018. A small heat shock protein 21 (sHSP21) mediates immune responses in Chinese oak silkworm *Antheraea pernyi*. Int. J. Biol. Macromol. 111: 1027–1031.

Liu, G., Z. Li, M. Yang, L. Lin, J. Liu, and M. Chen. 2020a. Functional characterization of a putative lipopolysaccharide-induced TNF-alpha factor (LITAF) from blood clam *Tegillarca granosa* in innate immunity. Fish Shellfish Immunol. 97: 390–402.

Liu, W., Y. Wang, Z. Leng, Q. Wang, X. Duan, Y. Luo, Y. Jiang, and L. Qin. 2020b. Nitric oxide plays a crucial role in midgut immunity under microsporidian infection in *Antheraea pernyi*. Mol. Immunol. 126: 65–72.

Love, M. I., W. Huber, and S. Anders. 2014. Moderated estimation of fold change and dispersion for RNA-seq data with DESeq2. Genome Biol. 15: 550.

Marchler-Bauer, A., C. Zheng, F. Chitsaz, M. K. Derbyshire, L. Y. Geer, R. C. Geer, N. R. Gonzales, M. Gwadz, D. I. Hurwitz, C. J. Lanczycki, *et al*. 2013. CDD: conserved domains and protein three-dimensional structure. Nucleic Acids Res. 41: D348–D352.

Moriwaki, Y., N. A. Begum, M. Kobayashi, M. Matsumoto, K. Toyoshima, and T. Seya. 2001. *Mycobacterium bovis* Bacillus Calmette-Guerin and its cell wall complex induce a novel lysosomal membrane protein, SIMPLE, that bridges the missing link between lipopolysaccharide and p53-inducible gene, LITAF(PIG7), and estrogen-inducible gene, EET-1. J. Biol. Chem. 276: 23065–23076.

Moriya, Y., M. Itoh, S. Okuda, A. C. Yoshizawa, and M. Kanehisa. 2007. KAAS: an automatic genome annotation and pathway reconstruction server. Nucleic Acids Res. 35: W182–W185.

Myokai, F., S. Takashiba, R. Lebo, and S. Amar. 1999. A novel lipopolysaccharide-induced transcription factor regulating tumor necrosis factor alpha gene expression: molecular cloning, sequencing, characterization, and chromosomal assignment. Proc. Natl. Acad. Sci. U. S. A. 96: 4518–4523.

Nakazawa, H., E. Tsuneishi, K. M. Ponnuvel, S. Furukawa, A. Asaoka, H. Tanaka, J. Ishibashi, and M. Yamakawa. 2004. Antiviral activity of a serine protease from the digestive juice of *Bombyx mori* larvae against nucleopolyhedrovirus. Virology. 321: 154–162.

Pan, M. H., X. J. Cai, M. Liu, J. Lv, H. Tang, J. Tan, and C. Lu. 2010. Establishment and characterization of an ovarian cell line of the silkworm, *Bombyx mori*. Tissue Cell. 42: 42–46.

Park, E. M., Y. O. Kim, B. H. Nam, H. J. Kong, W. J. Kim, S. J. Lee, I. S. Kong, and T. J. Choi. 2008. Cloning, characterization and expression analysis of the gene for a putative lipopolysaccharide-induced TNF-alpha factor of the Pacific oyster, *Crassostrea gigas*. Fish Shellfish Immunol. 24: 11–17.

Park, S. W., S. W. Kang, T. W. Goo, S. R. Kim, G. G. Lee, and S. Y. Paik. 2010. Tissue-specific gene expression analysis of silkworm (*Bombyx mori*) by quantitative real-time RT-PCR. BMB Rep. 43: 480–484.

Patro, R., G. Duggal, M. I. Love, R. A. Irizarry, and C. Kingsford. 2017. Salmon provides fast and bias-aware quantification of transcript expression. Nat. Methods. 14: 417–419.

Ponnuvel, K. M., H. Nakazawa, S. Furukawa, A. Asaoka, J. Ishibashi, H. Tanaka, and M. Yamakawa. 2003. A lipase isolated from the silkworm *Bombyx mori* shows antiviral activity against nucleopolyhedrovirus. J. Virol. 77: 10725–10729.

Selot, R., V. Kumar, S. Shukla, K. Chandrakuntal, M. Brahmaraju, S. B. Dandin, M. Laloraya, and P. G. Kumar. 2007. Identification of a soluble NADPH oxidoreductase (BmNOX) with antiviral activities in the gut juice of *Bombyx mori*. Biosci. Biotechnol. Biochem. 71: 200–205.

Silva, S. S., B. Kundu, S. Lu, R. L. Reis, and S. C. Kundu. 2019. Chinese oak tasar silkworm *Antheraea pernyi* silk proteins: current strategies and future perspectives for biomedical applications. Macromol. Biosci. 19: e1800252.

Smith, R. C., A. G. Eappen, A. J. Radtke, and M. Jacobs-Lorena. 2012. Regulation of anti-Plasmodium immunity by a LITAF-like transcription factor in the malaria vector *Anopheles gambiae*. Plos Pathog. 8: e1002965.

Sun, Y., Y. Jiang, Y. Wang, X. Li, R. Yang, Z. Yu, and L. Qin. 2016. The toll signaling pathway in the Chinese Oak Silkworm, *Antheraea pernyi*: innate immune responses to different microorganisms. Plos One. 11: e0160200.

Sun, Y., Y. Wang, W. Liu, J. L. Zhou, J. Zeng, X. H. Wang, Y. R. Jiang, D. H. Li, and L. Qin. 2017. Upregulation of a trypsin-like serine protease gene in *Antheraea pernyi* (Lepidoptera: Saturniidae) strains exposed to different pathogens. J. Econ. Entomol. 110: 941–948.

Tang, X., D. Metzger, S. Leeman, and S. Amar. 2006. LPS-induced TNF-alpha factor (LITAF)-deficient mice express reduced LPS-induced cytokine: evidence for LITAF-dependent LPS signaling pathways. Proc. Natl. Acad. Sci. U. S. A. 103: 13777–13782.

Tatusov, R. L., M. Y. Galperin, D. A. Natale, and E. V. Koonin. 2000. The COG database: a tool for genome-scale analysis of protein functions and evolution. Nucleic Acids Res. 28: 33–36.

Thompson, J. D., T. J. Gibson, and D. G. Higgins. 2002. Multiple sequence alignment using ClustalW and ClustalX. Curr Protoc Bioinformatics Chapter 2: Unit2.3.

UniProt-Consortium. 2019. UniProt: a worldwide hub of protein knowledge. Nucleic Acids Res 47: D506–D515.

Wang, X., H. Luo, and R. Zhang. 2018. Innate immune responses in the Chinese oak silkworm, *Antheraea pernyi*. Dev. Comp. Immunol. 83: 22–33.

Wang, P. H., D. H. Wan, L. R. Pang, Z. H. Gu, W. Qiu, S. P. Weng, X. Q. Yu, and J. G. He. 2012. Molecular cloning, characterization and expression analysis of the tumor necrosis factor (TNF) superfamily gene, TNF receptor superfamily gene and lipopolysaccharide-induced TNF-α factor (LITAF) gene from *Litopenaeus vannamei*. Dev. Comp. Immunol. 36: 39–50.

Xia, Q., D. Cheng, J. Duan, G. Wang, T. Cheng, X. Zha, C. Liu, P. Zhao, F. Dai, Z. Zhang, *et al*. 2007. Microarray-based gene expression profiles in multiple tissues of the domesticated silkworm, *Bombyx mori*. Genome Biol. 8: R162.

Zhang, J., Q. Li, G. Wei, L. Wang, C. Qian, Y. Sun, J. Tian, B. Zhu, and C. Liu. 2019. Identification and function of a lebocin-like gene from the Chinese oak silkworm, *Antheraea pernyi*. J. Invertebr. Pathol. 166: 107207.

Zhao, P., F. Xia, L. Jiang, H. Guo, G. Xu, Q. Sun, B. Wang, Y. Wang, Z. Lu, and Q. Xia. 2018. Enhanced antiviral immunity against *Bombyx mori* cytoplasmic polyhedrosis virus via overexpression of peptidoglycan recognition protein S2 in transgenic silkworms. Dev. Comp. Immunol. 87: 84–89.